Dispersion-Induced Chromatographic Waves

Steven L. Bryant, Clint Dawson, and Cornelius J. van Duijn

CRPC-TR99798
September 1999

Center for Research on Parallel Computation
Rice University
6100 South Main Street
CRPC - MS 41
Houston, TX 77005

Submitted November 1999

Dispersion-Induced Chromatographic Waves *

Steven L. Bryant[†§] Clint Dawson [†] and Cornelius J. van Duijn[‡]

November 18, 1999

Abstract

Motivated by field and laboratory observations of unusual wave propagation, we investigate the behavior of simple model problems involving transport with competitive adsorption of H^+ and a metal cation. In the absence of diffusion/dispersion, the model problem yields two shocks with the velocities expected from classical theory. In the presence of diffusion/dispersion, the solution exhibits an additional feature, a pulse of metal ion concentration that moves rapidly and independently of the metal ion shock. This 'fast wave' is associated with the pH shock in the simplest model problem studied here. Theoretical analysis of this problem yields a jump condition which numerical experiments confirm. Along with diffusion/dispersion, proton sorption/desorption appears to be prerequisite for this phenomenon. This extension of classical chromatography theory may explain several field and laboratory observations. One practical implication of this finding is the importance of accurate handling of diffusion and dispersion in numerical simulation of reactive transport problems. Another is that estimates of species migration based on simple theory, such as retardation factors, may fail to capture important features of the actual behavior.

Submitted to Industrial and Engineering Chemistry Research issue in recognition of Prof. Robert Schechter.

Keywords: reactive transport, chromatography, waves, sorption, dispersion, numerical methods

1 Introduction

Prefatory Remarks by S. Bryant. Reactive transport through porous media is but one of many areas of science and engineering to which Prof. Robert Schechter has made notable contributions. Having been privileged to work under Prof. Schechter's supervision, I would

*This work was supported in part by National Science Foundation grants DMS-9873326 and DMS-9805491, and by the Center for Research in Parallel Computation.

[†]Center for Subsurface Modeling - C0200; Texas Institute for Computational and Applied Mathematics; The University of Texas; Austin, TX 78712.

[‡]CWI; Amsterdam, The Netherlands.

[§]to whom correspondence should be addressed. *sbryant@ticam.utexas.edu*

venture that the aesthetic appeal of reactive transport has been at least as important a motivation for him as its numerous practical applications.

Chemical interactions between a flowing fluid phase and a stationary solid phase give rise to remarkably rich behavior. For example, reactive transport applications are among the few in which it is possible to get something for (almost) nothing. One can inject a fluid containing a species at a concentration C_J into an appropriate porous medium initially containing a solution with that species at concentration C_I, and extract from the medium (for a limited time) a fluid with species concentration exceeding both C_J and C_I. The modern-day ubiquity of chromatographic columns has perhaps dulled our appreciation of what would have been regarded a miraculous separation process in the not-too-distant past. And there is an element of beauty in the mathematics that underlies reactive transport, from the method of characteristics to the hodograph space of Rhee et al.

That so much can spring from so little – a couple of one-dimensional mass balance equations and a few chemical equilibrium expressions suffice – is remarkable. An admixture of wonder and serendipity stimulated the work described below, and my colleagues and I are delighted by the opportunity to include it in a celebration of Prof. Schechter.

2 Motivation

In this work we explore some of the mathematical and physical aspects of a fast-moving concentration peak that is distinct from the concentration fronts expected from classical theory. The original motivation for this work arose from simulations of metal cation migration through an aquifer from a high pH source. The simulations showed a 'hot spot' of metal ion moving at close to groundwater velocity. Given the strong affinity of the ferrous oxyhydroxide minerals in the aquifer for the cation at high pH, the metal should have remained in the immediate vicinity of the source for millenia. Exhaustive examination showed that the fast-moving peak was not an artifact, and indeed such movement was consistent with field observations showing significant migration within decades [1], [2].

Figure 1 illustrates this phenomenon in a simplified version of this problem. In this example, the strontium cation sorbs on a substrate S according to the following reaction

$$Sr^{++} + \mathrm{S} \rightarrow \mathrm{S}\text{-}Sr^{+} + H^{+} \tag{1}$$

and protons sorb according to

$$H^{+} + \mathrm{S} \rightarrow \mathrm{S}\text{-}H^{+} \tag{2}$$

with simple mass action equilibria for both reactions. The computed concentration profiles of Fig. 1 are at a time shortly before one pore volume of fluid has entered the medium, as the location of the tracer front indicates. The initial pH in the medium is 6 (i.e. $[OH^{-}] = 10^{-8}$) and the initial Sr concentration is taken to be 10^{-9}. The inlet (distance = 0) is held at $[Sr^{++}]$ = 10^{-4} and pH = 11 ($[OH^{-}] = 10^{-3}$). The strontium shock moves slowly in this example and induces a small drop in pH, associated with the displacement of H^{+} from the substrate. Downstream of this front is the pH shock, marking the consumption of sorbed H^{+} by the incoming hydroxyls. The two fronts satisfy expectations of classical theory outlined below:

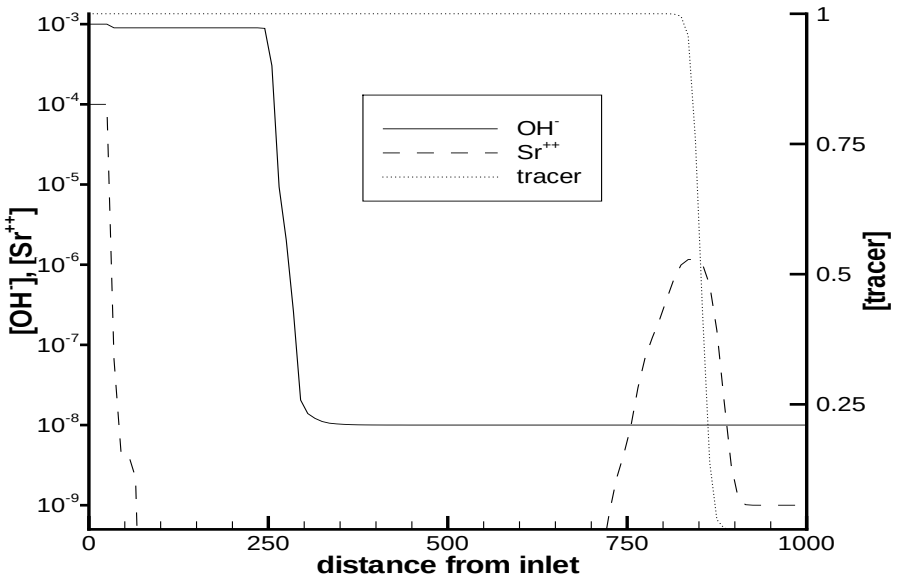

Figure 1: **Simulated injection of a pH 11 solution containing 10^{-4} M Sr and a conservative tracer into a porous medium at pH 6 yields a dispersion-induced wave of Sr. This wave moves rapidly, almost at interstitial fluid velocity, as indicated by the location of the tracer front. The slower-moving pH and Sr shocks, located at $d = 275$ and $d = 50$, respectively, behave as expected from classical chromatography theory. The sorption reactions (1)-(2) satisfy mass action equilibrium expressions with $K_{Sr} = 10^{-3.34}$ and $K_H = 10^{8.53}$.**

the concentration velocities for H^+ and Sr^{++} decrease in the downstream direction, so that shocks form, and the shock velocities satisfy the jump conditions. Far ahead of both shocks, moving almost at tracer velocity, is a peak of Sr. In this example the maximum concentration in the fast-moving pulse is about 1% of the inlet Sr concentration. The pulse induces a small decrease in pH, too small to be visible in this plot, corresponding to H^+ displaced from the substrate. The velocity of the pulse reflects the large concentration velocity (99.7% of fluid velocity) of the strontium cation at pH 6. This high velocity motivated the term 'fast wave', which we adopt for convenience in this paper, though it will be seen that a more descriptive term might be 'dispersion-induced wave'.

Flow of uranium-bearing solutions through bench-scale porous media shows analogous behavior under certain conditions [3]. For most cases, the cation propagates in a classical manner, but at high concentrations of injected cation, a relatively fast peak arises (cf. Figure 6d of [3]). This was attributed to interaction between the cation and H^+, since the cation concentration was high enough to affect pH in an unbuffered system. Barthelds [4] reported a similar phenomenon during injection of polymer solutions into porous media containing a second, immiscible fluid phase. A pulse of polymer at a concentration greatly exceeding the injected value reaches the exit of the porous medium rapidly. This behavior was attributed to competition between adsorption and excluded pore volume (pore space through which water but not polymer molecules can flow). It thus differs mechanistically from cation migration. Nevertheless the similarity is intriguing and raises questions of whether a more general class of such phenomena may exist.

The remainder of this section lays out the mathematical foundation for the reactive transport problem of interest. The metal ion migration problem originally involved dozens of aqueous chemical species, several of which adsorbed to multiple substrates according to a sophisticated two-layer surface complexation model [5]. This complexity hindered theoretical analysis of the phenomenon, and it was thus of interest to find the simplest possible chemical system that exhibited the fast-wave phenomenon. Subsequent sections describe two such systems and results obtained from them.

2.1 Mathematics of reactive transport in porous media

We describe flow with competitive adsorption of solutes on a substrate by means of a mass balance for chemical species. The balances includes accumulation, advection, diffusion/dispersion, reaction and source/sink terms. In general the reactions include speciation, precipitation/dissolution, oxidation/reduction, adsorption/desorption, ion exchange, radionuclide decay, and biodegradation. Mass transfer between the flowing phase and a stationary fluid phase can also be treated as a chemical reaction.

In the general case it is convenient to write the mass balances in terms of a basic set of chemical components. This set is the smallest one from which all other species in the problem can be created by means of chemical reactions (cf. [6]). In this case the accumulation term includes species in the flowing as well as in the stationary phases:

$$\phi \frac{\partial (C_{i_{tot}})}{\partial t} + \nabla \cdot (C_{i_{aq}} u - D \nabla (C_{i_{aq}})) = q_i \tag{3}$$

where ϕ is the porosity of the porous medium, $C_{i_{tot}}$ is the total concentration of component

i (sum of stoichiometric contributions from all species in all phases), $C_{i_{aq}}$ is the total flowing phase concentration of component i, u is the Darcy velocity field, D is the diffusion/dispersion tensor and q_i is the net source/sink term. An explicit rate of reaction term does not appear in the component mass balance. Accounting for all appearances of a component requires forming linear combinations of individual species concentrations, and the coefficients in those linear combinations are just the stoichiometric coefficients of the reactions. Thus the net rate of reaction of a chemical component vanishes.

In practice some reactions will reach thermodynamic equilibrium on a time scale shorter than the advection and dispersion time scales, while other reactions will be limited by kinetics. The equilibrium reactions impose relations between species concentration which can be written as a set of algebraic equations, or as a constrained optimization problem (minimization of Gibbs free energy subject to mass balance constraints). We adopt the former approach in this work.

Classical chromatography is a specialization of (3) to a single class of reactions, adsorption/desorption, for constant velocity flow in single spatial dimension in the absence of diffusion/dispersion:

$$\phi \frac{\partial(C_{i_{tot}})}{\partial t} + u \frac{\partial(C_i)}{\partial x} = 0 \tag{4}$$

where $C_{i_{tot}} = C_i + Z_i$, Z_i being the concentration of species i adsorbed on the substrate in moles per unit pore volume. The equilibrium relations for these reactions often take the form of Langmuir isotherms which determine the sorbed species concentrations as continuous, differentiable functions of the flowing phase concentrations:

$$Z_i = K_i C_i Z_{tot}/W \tag{5}$$

where Z_{tot} is the total concentration of adsorption sites on the substrate, K_i is an equilibrium constant measuring the affinity of species i for the substrate, and W is given by

$$W = 1 + \sum_i K_i C_i. \tag{6}$$

The total concentration of sites is also known as the adsorption capacity of the substrate, and we have

$$Z_{tot} = \sum_i (Z_i) + Z_o = \text{constant} \tag{7}$$

where Z_o is the concentration of vacant sites.

These equations were first treated by De Vault [7] and later by Rhee et al [8] and Helfferich and Klein [9], among others. The concept of concentration velocity arises naturally from this hyperbolic system. The mass balance equation can be rearranged to

$$\frac{\frac{\partial C_i}{\partial t}}{\frac{\partial C_i}{\partial x}} = -\frac{u}{\phi}\left(\frac{1}{1 + \frac{\partial Z_i}{\partial C_i}}\right) \tag{8}$$

and using the chain rule, one finds

$$v_{C_i} = (\frac{dx}{dt})|_{C_i} = \frac{v}{1 + \frac{\partial Z_i}{\partial C_i}} \tag{9}$$

where $v = u/\phi$ is the interstitial velocity. One simple wave arises for each sorbing species. The simple wave is a shock if concentration velocity decreases in the direction of travel, a rarefaction otherwise. When a shock arises, the differential mass balance is not well defined, and an integral mass balance can be written across the shock:

$$\frac{\Delta Z_1}{\Delta C_1} = \frac{\Delta Z_2}{\Delta C_2} = \ldots = \frac{\Delta Z_N}{\Delta C_N} = \frac{v}{v_{shock}} - 1, \tag{10}$$

where Δ indicates the jump in a quantity across the shock, N is the number of sorbing species and v_{shock} is the velocity of the front.

3 Model development

The classical theory of chromatography does not admit the 'fast wave' phenomenon. The simplest model problem that exhibits this behavior differs from the system (4)-(6) in two ways: the presence of diffusion/dispersion and the sorption of protons. The mathematical consequences of these features are that dispersion introduces a second derivative into the mass balances, and that the mass balance for protons is nonlinear in proton concentration.

To illustrate these differences, consider a competition for adsorption sites on a substrate S between protons H^+ and a cation denoted M^+:

$$M^+ + \mathrm{S} \rightarrow \mathrm{S}\text{-}M^+ \tag{11}$$

$$H^+ + \mathrm{S} \rightarrow \mathrm{S}\text{-}H^+. \tag{12}$$

The equilibrium expressions for these sorption reactions are taken to be the standard Langmuir type, (5)-(6). The dissociation of water imposes an equilibrium relationship between the concentrations of proton H^+ and hydroxyl anion OH^-:

$$C_{OH} = \frac{K_w}{C_H} \tag{13}$$

where K_w is the dissociation equilibrium constant for water.

The mass balance equation for the metal component reduces to

$$\phi \frac{\partial (C_M + Z_M)}{\partial t} + u \frac{\partial C_M}{\partial x} - D \frac{\partial^2 C_M}{\partial x^2} = 0. \tag{14}$$

The mass balance for protons must account for water dissociation and becomes

$$\phi \frac{\partial (C_H - C_{OH} + Z_H)}{\partial t} + u \frac{\partial (C_H - C_{OH})}{\partial x} - D \frac{\partial^2 (C_H - C_{OH})}{\partial x^2} = 0. \tag{15}$$

The quantity $C_H - C_{OH}$ is the acidity for this simple system [10].

We impose Riemann boundary conditions on this system. The initial state of the medium is at low pH ($C_H = 10^{-3}$) and background levels of metal ion concentration ($C_M = 10^{-12}$). The inlet is held at high pH ($C_H = 10^{-12}$) and relatively high metal concentration ($C_M = 10^{-3}$). Typical K_H and K_M are 10^4 and 10^3, respectively. The value of Z_{tot} depends on

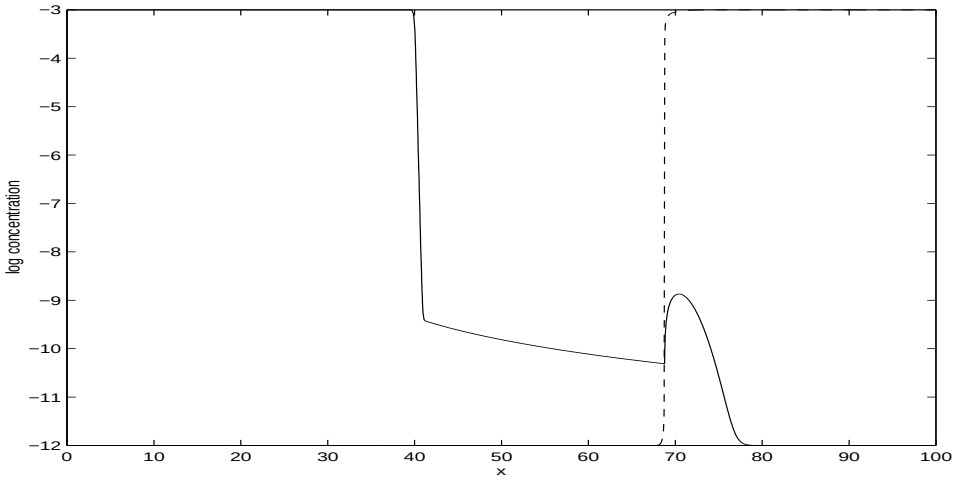

Figure 2: **Fast wave behavior for model system (14)-(15) in which protons and a metal ion compete for sorption sites. At a Peclet number of 100, the metal concentration (solid) exhibits a shock at $x = 40$ and a fast wave associated with the pH shock (dashed) at $x = 68$.**

the porous medium. Here it is taken to be of order 10^{-3} so that the shock velocities are convenient.

Classical theory indicates two simple waves for this problem, one for the proton and one for the metal ion. An example of the numerical results obtained below, Figures 2 and 3, shows that two such fronts do arise. The metal front is a shock lagging the pH front, which is also a shock. In addition to the expected metal front, a pulse of metal concentration is visible in the concentation profile of Fig. 2. This pulse is the fast wave, so called because it moves much faster than the metal shock.

The fast wave originates numerically as a slight 'kink' in the metal front in the vicinity of the pH shock. This is visible in Figure 3, where we have shown numerical solutions for metal and pH in the neighborhood of the pH front at early time. The metal front is beginning to separate into two waves, one which will lag well behind the pH front, and the fast wave. The fast wave occurs over a range of boundary conditions and equilibrium constants. In this model problem the fast wave travels with the pH shock, while in the example of (1)-(2) it travels independently of the pH shock. The existence and behavior of this pulse are the subject of the numerical and theoretical sections to follow.

3.1 Theoretical results

From the standpoint of chromatography theory, the fast wave is an anomaly. A central question early in this research was whether the wave had a mathematical basis, or whether it was merely a numerical artifact. In view of the importance of the pH shock to the existence of the fast wave in the system (14)-(15), we sought conditions that the metal concentration profile must satisfy in the vicinity of the pH shock.

One further simplification of the two-component model (14)-(15) facilitates a perturbation analysis of the behavior. In the numerical simulations, the pH front moves at essentially

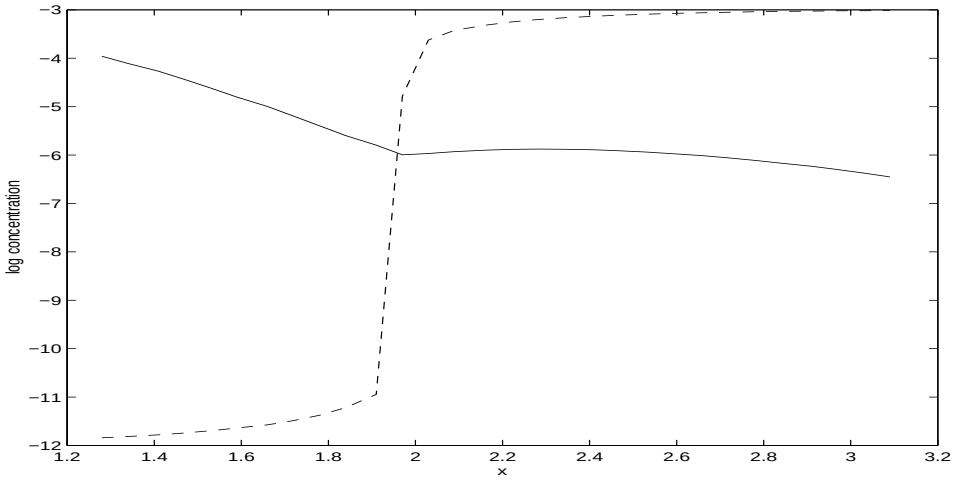

Figure 3: **Formation of the fast wave for the two-component model. At early time the metal profile (solid) shows a kink at the shock in proton concentration (dashed), which evolves into the fast wave.**

a constant velocity. Thus for the purpose of analysis we eliminate the proton mass balance (15) from consideration by assuming the pH front moves at velocity $a < 1$, with $C_H = 0$ to the left of $x - at = 0$ and $C_H = 1$ to the right of $x - at = 0$. For convenience we also set $K_H = 10$, $K_M = 1$, $Z_{tot} = 1$ and $u = 1$. This simplification yields a single-component problem expressed in terms of the metal concentration c:

$$\frac{\partial(c+z)}{\partial t} + \frac{\partial c}{\partial x} - D\frac{\partial^2 c}{\partial x^2} = 0, \quad x > 0, t > 0 \tag{16}$$

with

$$c(0,t) = 1, \quad t > 0 \tag{17}$$

and

$$c(x,0) = 10^{-12}, \quad x > 0 \tag{18}$$

where

$$z = \begin{cases} \frac{c}{1+c}, & x < at, \\ \frac{c}{11+c}, & x > at, \end{cases} \tag{19}$$

and a is assumed to be the velocity of the pH front. The key feature of this single-component problem is the influence of the discontinuity in the sorbed concentration z at $x - at = 0$.

In order to analyze the behavior of (16), we first consider the related model problem

$$\frac{\partial(1 + H(x-at))c}{\partial t} + \frac{\partial c}{\partial x} - D\frac{\partial^2 c}{\partial x^2} = 0, \tag{20}$$

in which the Heaviside function H captures the qualitative behavior of the discontinuous sorbed concentration. The perturbation analysis starts by replacing H by a smooth approximation $H_\epsilon(x-at) = \psi(\eta)$, where $\eta = \frac{x-at}{\epsilon}$ and $\epsilon > 0$ is small. Thus (20) becomes

$$(1+H_\epsilon)\frac{\partial c}{\partial t} + \frac{\partial H_\epsilon}{\partial t}c + \frac{\partial c}{\partial x} - D\frac{\partial^2 c}{\partial x^2} = 0. \tag{21}$$

Near $x = at$, we expand c:

$$c(x,t) \equiv u(\eta,t) = u_0(0,t) + \epsilon u_1(\eta,t), \tag{22}$$

which gives

$$\frac{\partial c}{\partial x} = \frac{\partial u_1}{\partial \eta} \tag{23}$$

$$\frac{\partial^2 c}{\partial x^2} = \frac{1}{\epsilon}\frac{\partial^2 u_1}{\partial \eta^2} \tag{24}$$

$$\frac{\partial c}{\partial t} = \frac{du_0}{dt} - a\frac{\partial u_1}{\partial \eta} + \epsilon\frac{\partial u_1}{\partial t}. \tag{25}$$

Substituting into (21) we find

$$\begin{aligned}(1+H_\epsilon)&\left\{\frac{du_0}{dt} - a\frac{\partial u_1}{\partial \eta} + \epsilon\frac{\partial u_1}{\partial t}\right\} \\ &- \frac{a}{\epsilon}\psi'\left\{u_0 + \epsilon u_1\right\} + \frac{\partial u_1}{\partial \eta} - \frac{D}{\epsilon}\frac{\partial^2 u_1}{\partial \eta^2} = 0.\end{aligned} \tag{26}$$

Collecting terms of order ϵ^{-1} gives

$$a\psi' u_0 + D\frac{\partial^2 u_1}{\partial \eta^2} = 0 \tag{27}$$

or

$$a\psi(\eta)u_0 + D\frac{\partial u_1}{\partial \eta} = \text{ constant}. \tag{28}$$

Since the solution c is classical for $x < at$ and $x > at$, this implies

$$D\left\{\frac{\partial c}{\partial x}(at^+,t) - \frac{\partial c}{\partial x}(at^-,t)\right\} + ac(at,t) = 0. \tag{29}$$

Thus the discontinuity in the accumulation term imposes a relation between the velocity of the discontinuity, the concentration profile and the dispersive flux in the vicinity of the discontinuity.

Returning now to (20), we write

$$c + z = c + \frac{c}{1+c} + \left\{\frac{c}{11+c} - \frac{c}{1+c}\right\}H(x-at) \tag{30}$$

$$\equiv f(c) + g(c)H(x-at). \tag{31}$$

Repeating the procedure above we find for the single-component problem that

$$D\left\{\frac{\partial c}{\partial x}(at^+,t)-\frac{\partial c}{\partial x}(at^-,t)\right\}+ag(c(at,t))=0. \tag{32}$$

Thus the effect of the pH shock is to induce a discontinuity in the metal concentration gradient. The consequent jump in the dispersive flux of metal ion at the pH shock balances the rate at which metal must be supplied to advance the upstream sorbed concentration. Since $g(c)$ is negative, a metal concentration profile that decreases as it approaches the shock must increase downstream of the shock. The kink in the profile is therefore not a numerical artifact but rather a consequence of the pH shock in the presence of dispersion.

3.2 Numerical results.

A numerical approximation of the single-component problem (16) was implemented, and from this model we checked the condition (32) numerically. Figure 4 shows plots of the numerical solution in a neighborhood of the point $x = at$ at various times. These figures demonstrate the formation of a 'kink' in the solution, with the slope of the function on either side of the kink varying according to (32). In these runs, we took $D = 1.0$ and $a = 11/13$. The quantity on the left side of (32) was also computed numerically at each time and was found to be on the order of 10^{-5}.

The single-component model thus provides reasonable assurance of the physical validity of the fast wave. We then implemented a numerical approximation to the two-component model (14)-(15) in order to study its fast-wave behavior in more detail. The approximation is based on a simple finite difference scheme. We divide the interval $0 \le x \le L$ into J intervals $0 = x_{1/2} < x_{3/2} < \ldots < x_{J+1/2} = 1$ and choose a time-step $\Delta t > 0$. On each interval $[x_{i-1/2}, x_{i+1/2}]$ and each time step t^n we approximate C_M and C_H by constants $C^n_{M,i}$ and $C^n_{H,i}$. The finite difference discretization of (14) is then

$$\partial_t(C^n_{M,i}+Z^n_{M,i})+u\partial^u_x C^n_{M,i}-D\partial^2_x C^n_{M,i}=0, \tag{33}$$

where

$$\partial_t g^n = \frac{g^n-g^{n-1}}{\Delta t} \tag{34}$$

$$\partial^u_x g_i = \frac{g_i-g_{i-1}}{x_{i+1/2}-x_{i-1/2}} \tag{35}$$

$$\partial^2_x g_i = \frac{\frac{g_{i+1}-g_i}{x_{i+1}-x_i}-\frac{g_i-g_{i-1}}{x_i-x_{i-1}}}{x_{i+1/2}-x_{i-1/2}} \tag{36}$$

and

$$Z^n_{M,i}=Z(C^n_{M,i},C^n_{H,i}). \tag{37}$$

A similar equation to (33) is used for $C^n_{H,i}$. These coupled nonlinear equations are solved using Newton iteration. The same approximating scheme was used to solve the one-component model (16).

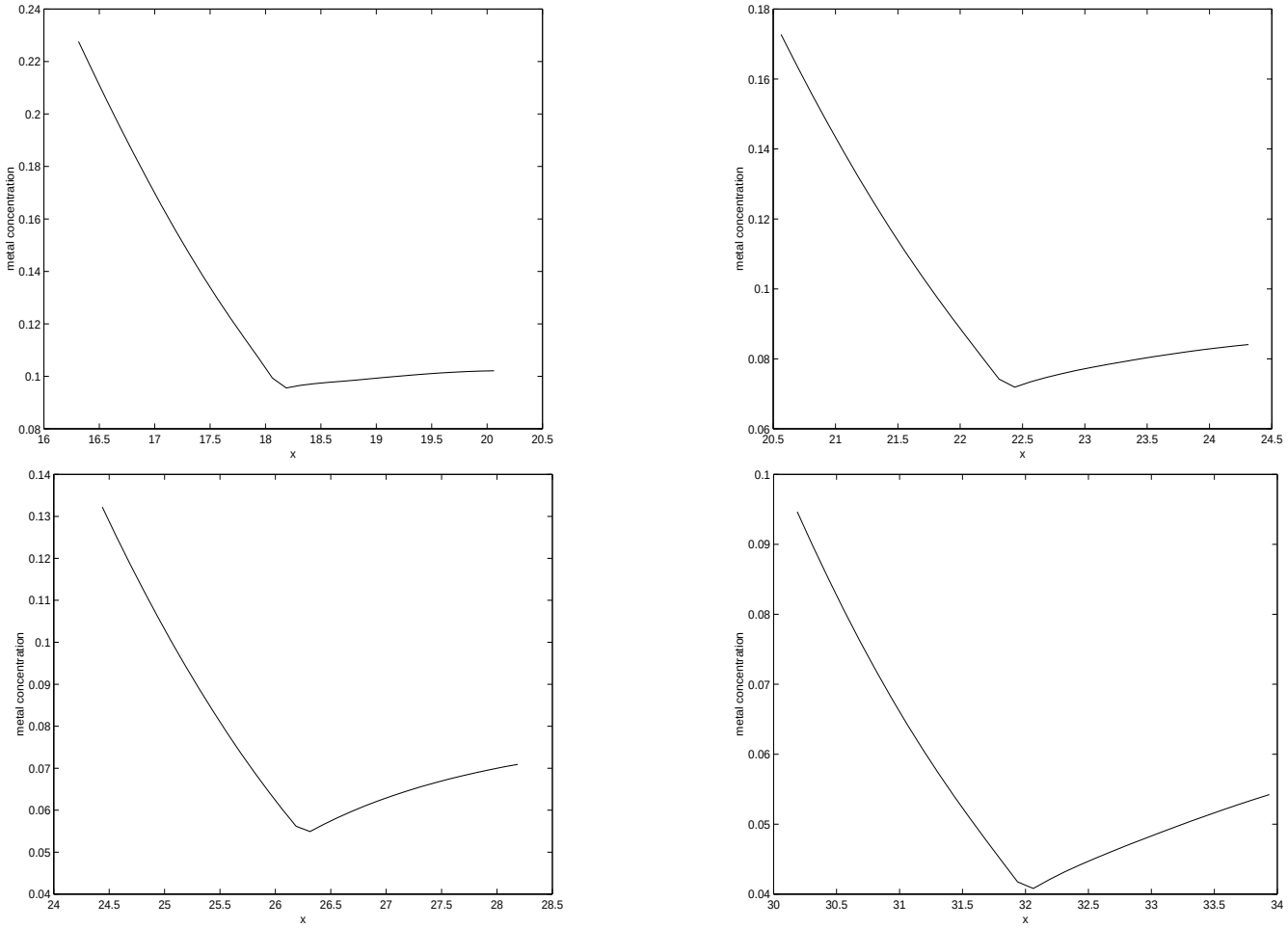

Figure 4: **Numerical solution near $x = at$ for single-component model (16). The solution satisfies the independently derived jump condition (32). The kink in the metal concentration profile becomes more pronounced as the pH front advances.**

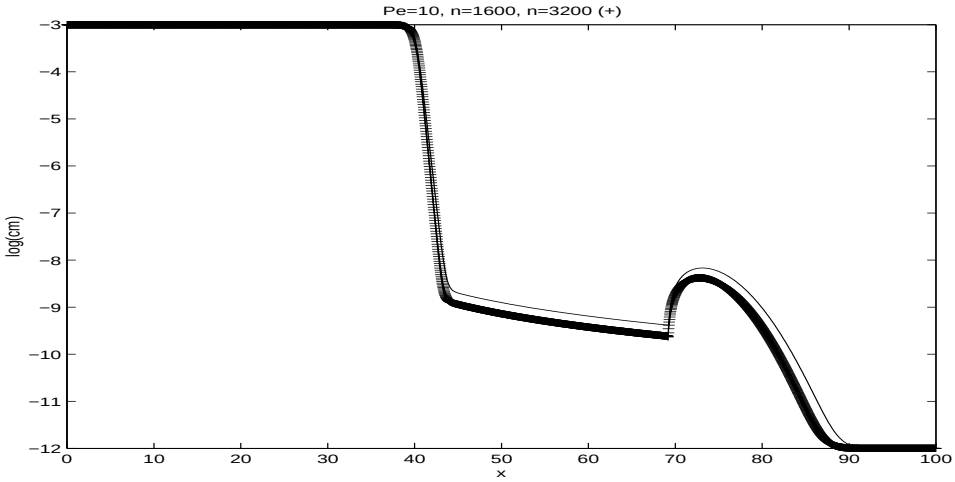

Figure 5: **Numerical solution, $log(C_M)$ vs. x for $D = 0.1$ at $t = 80$. Doubling the grid resolution reduces the contribution of numerical dispersion to the mass in the fast wave.**

The numerical scheme has been used to study the fast wave behavior under many different scenarios. An interesting feature of the fast wave is its behavior for different Peclet numbers. In a representative case the initial state of the medium is $C_H = 10^{-3}$ and $C_M = 10^{-12}$. The inlet is held at high pH ($C_H = 10^{-12}$) and relatively high metal concentration ($C_M = 10^{-3}$). The values of K_H and K_M are 10^4 and 10^3, respectively, $Z_{tot} = 10^{-3}$ and $K_W = 10^{-14}$. In Figure 5, we plot the approximation to C_M for $D = .1$, $L = 100$, at time $t = 80$. Two different solutions are plotted to show the effect of grid refinement, one with 1600 subintervals ($J = 1600$) and one for 3200 subintervals. For comparison, we have plotted the same solution for $D = .01$ in Figure 6. Note that the width and height of the fast wave decrease as D decreases, indicating that the characteristics of the wave are functions of diffusion/dispersion. In fact, as $D \to 0$, we have observed that the fast wave slowly vanishes under grid refinement, as seen in Figure 7. The fact that it appears at all when $D = 0$ is an effect of numerical diffusion. Under Riemann boundary conditions, the metal and pH shocks coexist at the inlet at time zero. Only an extraordinarily refined finite difference solution will resolve the two shocks at early times, and thus typical numerical solutions will artificially smear the profiles.

4 Discussion

The theoretical and numerical findings above demonstrate that the fast wave is a bona fide feature of the reactive transport problem, not an artifact, and that it occurs over a range of boundary conditions and chemical systems. Although rigorously established necessary and sufficient conditions for the fast wave are not yet available, two features seem to be necessary. One is the sorption of protons (or hydroxyls) on the substrate. Because of the dissociation of water, the mass balance equation for protons includes a nonlinear term in proton concentration. It is not yet clear how the nonlinearity in the proton mass balance

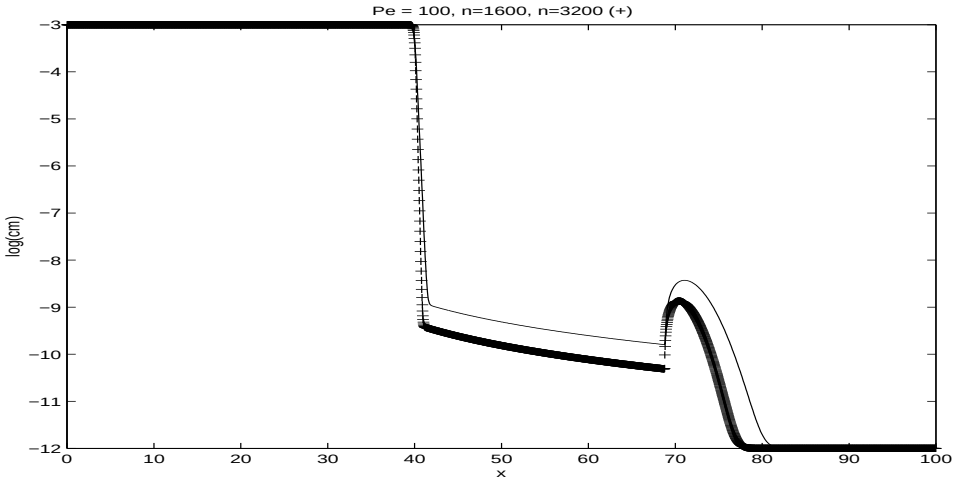

Figure 6: **Numerical solution, $log(C_M)$ vs. x for $D = 0.01$ at $t = 80$. Compared to the higher-dispersion case ($D = 0.1$) of Fig. 5, numerical dispersion plays a larger role. The mass in the fast wave is considerably smaller than in the higher-dispersion case.**

equation induces a peak in the concentration profile of the other sorbing species, but it does appear to be an intrinsic part of the phenomenon. If the proton is replaced in the model problems above by any other cation, then there is no such nonlinearity in the corresponding mass balance, and we have not observed the fast wave in such problems.

The other essential feature is the presence of dispersion. The jump condition for the metal ion concentration, (32), degenerates in the absence of dispersion. Furthermore the two shocks of pH and metal concentration satisfy the zero-dispersion mass balance equations. The fast wave is thus essentially a consequence of dispersion; it does not exist in the absence of dispersion, as demonstrated numerically in Fig. 7.

While proton/hydroxyl sorption appears essential to the existence of fast waves, the character of fast waves reflects the details of the sorption reactions. In the simplest chemical system (11)-(12) the fast wave travels with the pH shock. The sorption reactions (1)-(2) are slightly more complex, with the proton concentration appearing explicitly in the metal sorption reaction. In this case the fast wave travels independently of the pH front, as seen in Fig. 1. Still more complex sorption reactions, e.g. accounting for contributions of surface charge, exhibit fast waves similar to that of Fig. 1.

The initial conditions also influence the existence and behavior of the dispersion-induced wave. In the chemical system of (1)-(2) the dilute concentration velocity of metal ion depends strongly on pH. In the chemical system of Figure 1, the inlet conditions produce a peak that propagates very rapidly (99.7% of tracer velocity) ahead of the pH front, where the pH is at its initial value of 6. When the initial pH is 7, the dispersion-induced wave is broader, exhibits a smaller peak concentration, and does not propagate as rapidly, Figure 8a. This is consistent with the lower metal concentration velocity (79% of tracer velocity) at pH 7. When the initial pH is 8, the metal concentration velocity is much lower (4.6% of tracer velocity), and no dispersion-induced wave can be sustained, Figure 8b.

These considerations suggest an empirical explanation for the existence of the dispersion-

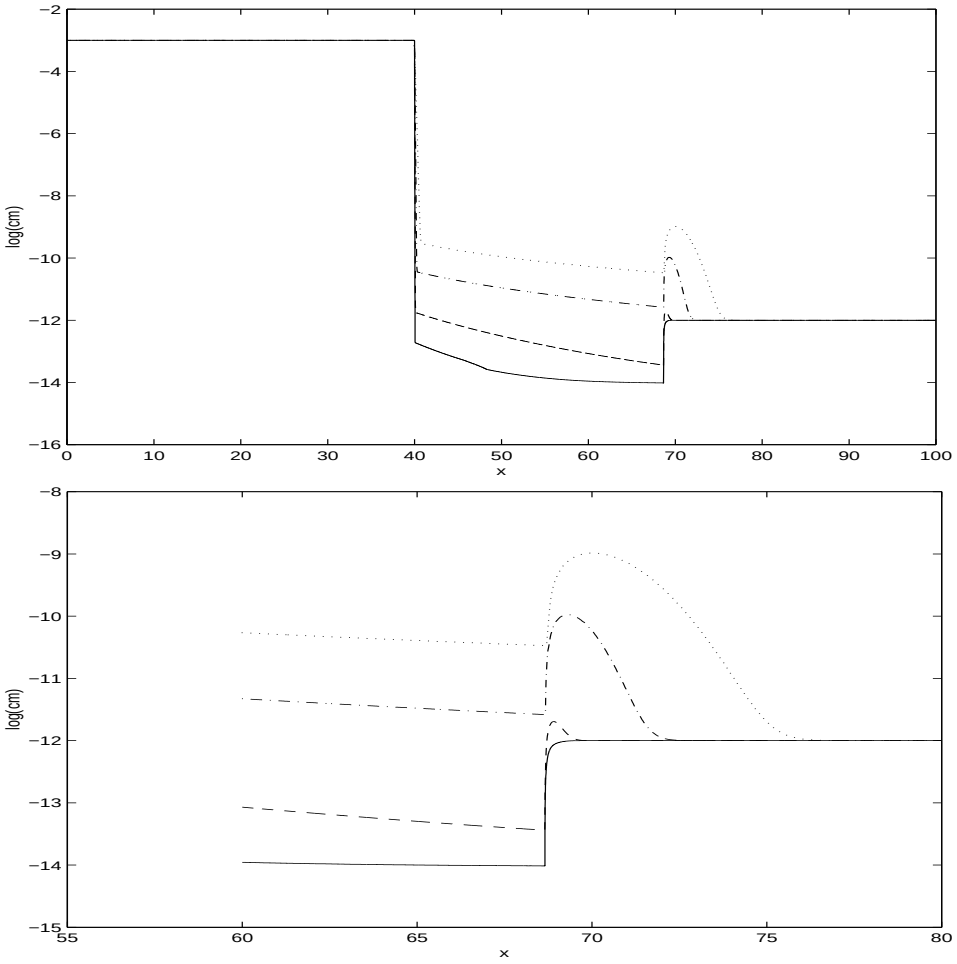

Figure 7: **Numerical solution, $log(C_M)$ vs. x for $D = 0.0$ at $t = 80$; 3200 (dotted), 9600 (dash-dot), 20000 (dashed) and 40000 (solid) grid blocks. The upper panel shows the entire concentration profile, the lower panel the detail around the fast wave. Numerical dispersion in all but the highest resolution simulation is sufficient to induce the fast wave.**

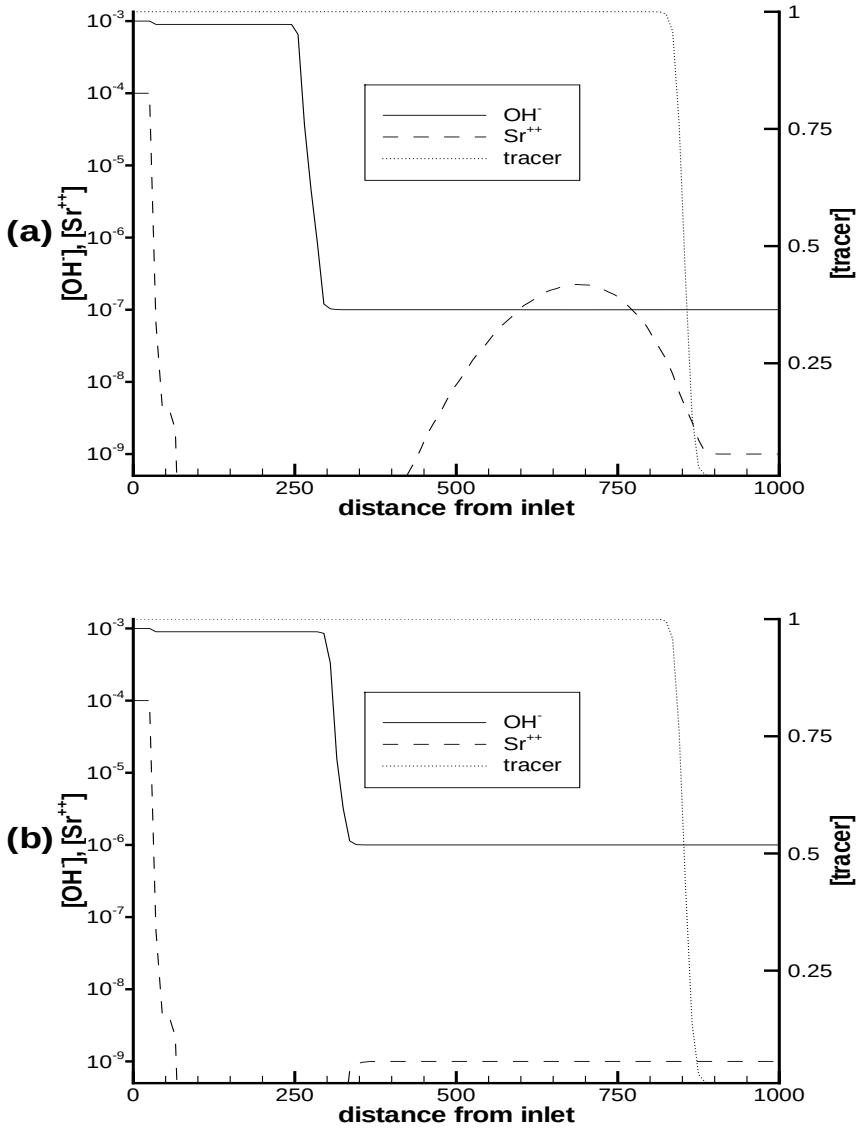

Figure 8: **The initial conditions in the porous medium influence the behavior of the fast wave for the sorption reactions (1)-(2). (a) Injection of pH 11 solution containing 10^{-4} M Sr and a conservative tracer into a porous medium initially at pH 7 yields a smaller peak concentration that moves more slowly than when the initial pH is 6, cf. Fig. 1. (b) When the initial pH is 8, the metal concentration velocity is too low to maintain a fast wave.**

induced wave. For Riemann boundary conditions, both the pH shock and the metal shock coexist at the inlet at time zero. For some period of time, until these shocks are sufficiently separated, dispersion can transfer metal cation into the lower pH region ahead of the pH shock. Once there, the higher concentration velocity ensures that the metal concentration propagates as a separate entity. In the absence of dispersion, there is no mechanism for establishing the metal ahead of the pH front, and no fast wave is possible.

If dispersive flux of metal across the pH front is the mechanism for generating the fast wave, then the wave should weaken if the pH front is initiated farther from the metal source (the high metal concentration upstream of the metal shock). This prediction was tested numerically in the following manner. The initial condition of the medium was altered in a small region at the inlet. This region was set at the same pH as the injected solution, but contained only background metal concentrations. Consequently, at time zero the pH front starts not at the inlet, but at the boundary between the altered zone and the rest of the medium. Thus the metal front and pH fronts never coincide, as they do in the Riemann problem, and there should be less flux of metal into the region ahead of the pH front.

Figure 9 illustrates this experiment for an altered region extending 0.02 pore volumes (PV) into the medium. The finite difference grid was spaced at 0.01 PV, ensuring numerical resolution of separate pH and metal fronts. In the absence of dispersion, no metal can move into the region ahead of the pH front. Thus the metal concentration profile exhibits only the classical shock upstream of the pH front and then rises to the value initially present in the medium. In the presence of dispersion, however, a flux of metal ion is possible across the gap between the metal and pH fronts. The resulting concentration profile exhibits the fast-moving peak. The larger the dispersion coefficient, the greater the concentration of metal in the peak.

A similar conclusion follows from consideration of the shock velocities. The slower the pH shock moves, the longer the time before the dispersive flux from the metal source into the region downstream of the shock is small. Thus the mass of cation in the fast-moving wave is larger for slower pH shocks, and the peak concentration may also be larger, depending on the degree of dispersion. Numerical experiments confirm this prediction. Peak concentrations as high as 20% of the injected metal concentration have been observed. The shock velocities depend on both the initial conditions and the boundary conditions and are inversely proportional to Z_{tot}, the total concentration of sites. Thus the magnitude of the fast wave is a complicated function of the chemical system, the porous medium, the boundary and initial conditions, and level of diffusion/dispersion.

The fast wave differs qualitatively from mixed waves that are familiar from multiphase flow. The latter typically comprise a shock trailed by a rarefaction and occur for suitably complicated fractional flow curves (at least one inflection point) and appropriate boundary conditions. Exactly analogous behavior arises in the reactive transport problem if the adsorption isotherm contains an inflection point. The Langmuir isotherms used in the examples presented above do not have inflection points. If the proton sorption isotherm is written in terms of the acidity $C_H - C_{OH}$, it does become sigmoidal. But the fast wave arises in the metal concentration, not in the proton or hydroxl concentrations, and the metal isotherm has no mixed wave character. In any event, if the phenomenon were a consequence only of the shape of the isotherm, it would occur regardless of the presence/absence of dispersion. Mixed waves exist independently of dispersion, whereas the fast wave does not.

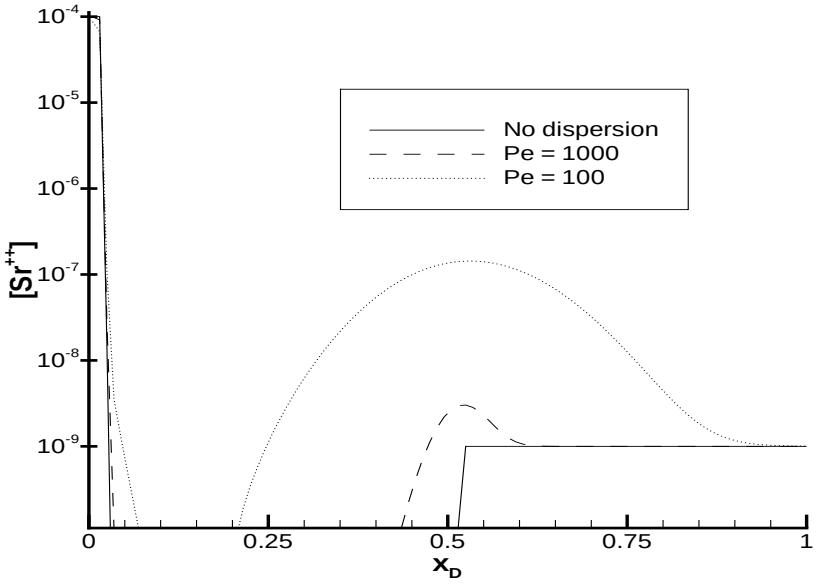

Figure 9: **The physical basis for the fast wave is dispersive flux of metal across the pH shock, illustrated here by a numerical experiment for the chemical system (1)-(2). Computed metal concentration profiles are shown for different levels of dispersion after 0.5 PV injection. The boundary and initial conditions are identical to those for Figure 1, except that the medium extending 0.02 PV from the inlet initially contains pH 11 solution containing only background metal concentration. Thus the pH shock and metal shock are always separated by at least 0.02 PV distance, whereas in the Riemann problem the two shocks coincide at the inlet at time zero. The greater the dispersion coefficient, the greater the mass of metal carried in the fast wave. In the absence of dispersion the fast wave does not exist, because there is no mechanism for moving the metal ahead of the pH front.**

The existence of dispersion-induced waves has implications for various applications. Clearly an analysis of a problem based on classical (zero-dispersion) theory may neglect an important feature of the behavior. Advection schemes which handle dispersion accurately will be crucial for simulating the behavior of such systems.

Qualitatively we have observed the dispersion-induced wave in problems that are much more complex chemically, as long as proton (or hydroxyl) adsorption occurs. Indeed the first problem in which we saw this behavior involved amphoteric substrates which can be protonated and deprotonated, cation sorption reactions that required simultaneous deprotonation, and sorption energetics computed from a generalized two-layer model [5]. There were multiple sorbing cations which underwent more than a dozen speciation reactions, many of which involved protons or hydroxyls. The mass balance equation for protons was correspondingly more complicated than the model system given above. Yet the salient feature of a rapidly moving concentration peak still arose for one of the sorbing metal ions.

5 Conclusions

Classical chromatography theory explains the migration of sorbing species in terms of simple waves, the character of which is determined by the concept of concentration velocities. For certain problems involving flow and competitive adsorption, a novel type of wave arises which cannot be explained in classical terms. A signature feature of this type of wave is the relatively rapid migration of a concentration peak, whence the informal name 'fast wave'.

Empirically, the necessary conditions for fast waves are nonzero diffusion/dispersion and competitive adsorption of protons (or hydroxyls). The details of the chemical system do not appear to be critical; the phenomenon arises for very simple two-component systems as well as for multicomponent systems with speciation reactions and sophisticated sorption equilibria. It appears that the fast wave can occur for any sorbing species except protons (or hydroxyls).

The physical basis of the fast wave is the diffusion/dispersion of a sorbing species through a proton concentration shock. The diffusive/dispersive flux establishes this species downstream of the pH shock, and a fast wave forms if the species concentration velocity is sufficiently high at the conditions prevailing downstream of the shock.

Theoretical analysis of an idealized model problem establishes a jump condition at the pH shock that the sorbing species concentration profile must satisfy. Numerical solutions satisfy this condition, and numerical experiments for simple two-component (metal cation and proton) sorption confirm the fundamental role of diffusion/dispersion in this phenomenon.

The theoretical and numerical results are consistent with field and laboratory observations of rapid cation migration in the presence of large variations in pH. For this class of problems, careful handling of diffusion and dispersion is critical for accurate simulation of reactive transport. Moreover, analysis based on classical theory (which does not account for dispersion) or upon simplifications of such theories (e.g. lumped retardation factors) will fail to capture an important aspect of such problems.

References

[1] Saunders, J. and Toran, L. Modeling of radionuclide and heavy metal sorption around low- and high-pH waste disposal sites at Oak Ridge, Tennessee. Appl. Geochem. 1995, 10, 673.

[2] Toran, L., Bryant, S., Saunders, J., and Wheeler, M. Sr Mobility Under variable pH: Application of a coupled Geochemistry and Transport Model. Ground Water 1998, 36, 404.

[3] Kohler, M., Curtis, G., Kent, D. and Davis, J. Experimental investigation and modeling of uranium(VI) transport under variable chemical conditions. Water Resources Research 1996, 32, 3539.

[4] Barthelds, A. The influence of inaccessible and excluded pore volume on polymer flooding. Ph.D. dissertation. Delft University of Technology, 1998.

[5] Dzombak, D. and Morel, F. Surface complexation modeling; Wiley: New York, 1990.

[6] Smith, W. and Missen, R. Chemical reaction equilibrium analysis: theory and algorithms; Wiley: New York, 1982.

[7] De Vault, D. The theory of chromatography. J. Am. Chem. Soc. 1943, 65, 532.

[8] Rhee, H.-K., Aris, R. and Amundson, N. On the theory of multicomponent chromatography. Proc. Roy. Soc. Lond. 1970, 267, 419.

[9] Helfferich, F. and Klein, G. Multicomponent chromatography; Marcel Dekker, New York, 1970.

[10] Scheidegger, A., Buergisser, C., Borkovec, M., Sticher, H., Meeussen, H. and van Riemsdijk, W. Convective transport of acids and bases in porous media. Water Resources Research 1994, 30, 2937.